International Journal of Biological Macromolecules 323 (2025) 146632

Contents lists available at ScienceDirect

International Journal of Biological Macromolecules

journal homepage: www.elsevier.com/locate/ijbiomac

SUMO-2 activity is inhibited by non-covalent interactions with the Aβ peptide: an exploration of potential pathogenic mechanisms in Alzheimer's disease

Valeria Ciaffaglione [a], Giulia Grasso [a], Valeria Lanza [a], Michele Francesco Maria Sciacca [a], Stefania Zimbone [a], Maria Laura Giuffrida [a], Claudio Iacobucci [b], Alessio Di Ianni [c], Damiano Calcagno [d], Giuseppe Grasso [e], Andrea Alloni [f], Franca Orsini [f], Paul Fraser [g], Luana Fioriti [f], Danilo Milardi [a,*]

[a] Istituto di Cristallografia, Consiglio Nazionale delle Ricerche, Sede Secondaria di Catania, Via Paolo Gaifami 18, 95126 Catania, Italy
[b] Dipartimento di Scienze Chimiche e Fisiche, Università degli Studi dell'Aquila, via Vetoio, Coppito 67100, L'Aquila, Italy
[c] Human Technopole, V.le Rita Levi Montalcini 1, 20157 Milan, Italy
[d] IRCCS-Fondazione Bietti, Rome, Italy
[e] Dipartimento di Scienze Chimiche, Università degli Studi di Catania, V.le Andrea Doria 6, 95125 Catania, Italy
[f] Istituto di Ricerche Farmacologiche Mario Negri IRCCS, Via Mario Negri, 2, 20156 Milano, Italy
[g] University of Toronto, Tanz Centre for Research in Neurodegenerative Diseases and Department of Medical Biophysics, Toronto, Ontario M5T 2S8, Canada

ARTICLE INFO

Keywords:
Aggregation
Ubiquitin
Neurodegeneration
Amyloid
Proteinopathies

ABSTRACT

SUMOylation is a post-translational modification involving the addition of SUMO isoforms to target proteins and plays a role in various biological processes, including neurodegenerative diseases and ocular pathologies. This study investigates the interaction between SUMO-2 and amyloid (Aβ) peptides, key contributors to Alzheimer's disease, using techniques like cross-linking mass spectrometry, surface plasmon resonance and biolayer interferometry. Data are available via ProteomeXchange with identifier PXD066055. The results show that Aβ1-40 and Aβ1-42 bind more strongly to SUMO-2 than to ubiquitin, with binding driven by specific hydrogen bonds and hydrophobic interactions. SUMO-2 was found to inhibit the conversion of Aβ into β-sheet structures and impede Aβ aggregation. Notably, Aβ competes with SUMO-2 canonical substrates for binding, completely hindering SUMOylation reactions in vitro. Identifying SUMO-2/Aβ1-42 adducts in cellular extracts and live cells further highlights the biological significance of these interactions. Overall, the findings indicate that Aβ peptides impair SUMO-2 function, pointing to the necessity for more research on the implications of SUMOylation in Alzheimer's disease.

1. Introduction

Alzheimer's disease (AD), the predominant form of dementia, is a neurodegenerative disorder marked by cognitive decline, memory loss, and behavioral changes, culminating in a loss of independence and, eventually, death. Its etiology remains complex and not entirely elucidated. A key histological feature of AD involves the deposition of extracellular plaques enriched in Aβ peptides produced by neuronal cells [1]. Aβ peptides, containing 40 or 42 amino acids (Aβ1-40 and Aβ1-42), are produced during the sequential hydrolytic cleavage of the amyloid precursor protein (APP) [2–5] by the proteases β- and γ-secretase [6]. Intracellular Aβ aggregates in AD brains have been identified using antibodies that specifically target Aβ1-40 and Aβ1-42 [7]. Further studies have shown that Aβ species of different lengths from intracellular regions can be relocated to the nucleus [8]. Aβ1-42 has a greater tendency to aggregate than Aβ1-40 because it contains two extra hydrophobic residues (isoleucine and alanine) at the C-terminus [9]. Nevertheless, Aβ1-40 is more prevalent, produced in a molar ratio of 9:1 compared to Aβ1-42 [10]. The "amyloid hypothesis" posits that the abnormal accumulation of these peptides in the brain plays a pivotal role in AD [11].

Even though it is widely acknowledged as the prominent theory for AD, the amyloid hypothesis falls short of fully elucidating the pathology.

* Corresponding author.
E-mail address: danilo.milardi@cnr.it (D. Milardi).

https://doi.org/10.1016/j.ijbiomac.2025.146632
Received 5 June 2025; Received in revised form 16 July 2025; Accepted 5 August 2025
Available online 18 August 2025

Indeed, numerous clinical trials targeting Aβ aggregation have failed to halt or reverse disease progression, casting doubt on its central role [12]. Furthermore, discrepancies arise as some individuals with substantial amyloid plaque accumulation remain unaffected by AD, while some patients with the disease lack extensive plaques, suggesting amyloid aggregation could be a symptom rather than the root cause, with other factors, such as ineffective post-translational modifications (PTMs), metal ions, [13] lipids and oxidative stress [14] playing significant roles in disease mechanisms [15,16].

SUMO, an acronym for Small Ubiquitin-like Modifier, is a small protein involved in PTMs that activates diverse cellular processes, including protein stability, protein-protein interactions, DNA repair, ocular development and pathology [17] and gene expression regulation [18,49]. In analogy to Ubiquitin, the SUMO pathway entails the covalent attachment of SUMO proteins to target proteins, termed SUMOylation, a reversible post-translational modification that governs protein function, localization, and interactions [19,20]. While Ubiquitin and the Ubiquitin conjugation pathway are distributed throughout the cell [21], the components of the SUMO conjugation machinery are known to be primarily located in the nucleus [22]. However, recent findings suggest that SUMO proteins, as well as SUMO ligases and de-conjugating enzymes, reside within synapses, as demonstrated by their colocalization with synaptophysin and postsynaptic density protein 95 (PSD95) [23].

Despite their quite distinct functions and sequences, SUMO and Ubiquitin, are marked by structural similarities, featuring a common 3D structure referred to as a "beta-grasp fold" comprising a tightly twisted sheet of β-strands embraced by an α helix [24]. However, their surface properties diverge, leading to distinct interaction characteristics with other proteins. A notable shared feature is the presence of a C-terminal diglycine motif in both proteins, essential for their covalent attachment to targets. Activation of this C-terminal tail occurs through a sequence of enzymatic steps involving activating (E1), conjugating (E2), and ligating (E3) enzymes, enabling the formation of an isopeptide bond with lysine residues in the protein substrates. This mechanism is commonly observed in both SUMOylation and ubiquitination processes [25].

In humans, three isoforms of the SUMO protein exist: SUMO-1, SUMO-2, and SUMO-3. While SUMO-2 and SUMO-3 exhibit structural similarity with nearly 97 % sequence identity and are commonly treated as members of a single subfamily, SUMO-1 shares only approximately 50 % sequence identity with SUMO-2 and SUMO-3 [26]. These isoforms possess distinct cellular targets and functions [27]. Recent investigations indicate a plausible association between abnormalities in the SUMO pathway and AD pathogenesis, and low levels of SUMOylation have been linked to Aβ accumulation in neuronal cells [27–30]. Particularly, previous reports demonstrate the presence of SUMO-2 immunoreactivity in neurons within the AD brain compared to those in unaffected individuals [31]. Engagement with SUMO-2 might affect the structure or function of amyloid proteins, potentially altering their aggregation pattern or enhancing their degradation [27]. However, the precise mechanisms through which SUMO-2 influences amyloid peptide metabolism have not yet been reported.

To enhance our understanding of AD mechanisms and address gaps in the literature, here we investigate the non-covalent interactions between Aβ and SUMO-2. Specifically, our focus is on elucidating the affinity constants, contact surfaces, and structural details of the SUMO-2/Aβ complex, along with Aβ ability to inhibit SUMOylation. The outcomes of these experiments may provide insights into the role of SUMO in AD, offering potential targets for therapeutic species design.

2. Materials and methods

2.1. Chemicals

Aβ1-40 (Hexafluoroisopropanol or HFIP treated) was purchased from Bachem; phosphate buffer saline, (PBS) Tween 20, and all other chemicals were purchased from Sigma-Aldrich. Carboxy-methyl-dextran (CMD) and functionalized gold sensor chip (CDL) was obtained from Sartorius Corporation. Aβ1-42 (HFIP-treated), Aβ1-40 trifluoroacetate salt, BiotinylatedAβ1-40) trifluoroacetate salt and Biotinylated Aβ1-42 ammonium salt were purchased from Bachem AG (Prodotti Gianni). Ubiquitin was purchased from Giotto Biotech s.r.l.

2.2. SUMO-2 recombinant protein expression and purification

The human SUMO-2 ORF (NCBI Reference Sequence: NM_006937.4) was prepared as previously described [32]. Briefly, SUMO2 was inserted into the pET-28 expression plasmid using *Xba*I and BamHI restriction sites, with a leader sequence (HHHHHHPMSDYDIPTTENLYFQGA) with a TEV cleavage site (GA) and hexa-His tag immediately N-terminal to the SUMO-2 sequence. Protein was expressed in *E. coli* grown in Terrific Broth containing antibiotic (50 μg/ml kanamycin) with induction (1 mM IPTG) at 37 °C for 4 h. Cell pellets were resuspended in buffer (20 mM HEPES, 300 mM NaCl, 20 mM imidazole; pH 7.4) and lysed by sonication. Lysates were clarified by centrifugation (10,000 *g*) and applied to a nickel affinity column (Qiagen Superflow). Bound protein was washed with buffer containing 40 mM imidazole and eluted with 300 mM imidazole. Eluates were pooled and buffer exchanged by dialysis to PBS with 1 mM dithiothreitol. Protein was concentrated using Amicon Ultra-15 with a molecular weight cut-off of 10 kDa and purified by size exclusion column (Cytiva Superdex 75) in PBS. Fractions containing purified SUMO-2 were sterile filtered with Acrodisc units with Mustang E membrane and aliquots snap frozen in liquid nitrogen then stored at −80 °C. Quality control and purity of the isolated protein were assessed by SDS-PAGE and immunoblotting (see Fig. S1 in Supplementary information). The recombinant SUMO-2 was found to be a single band as determined by Coomassie Blue staining which was confirmed by immunoblotting using an anti-SUMO-2 rabbit polyclonal antibody (Millipore Sigma, cat. SAB4200190; dilution 1:1000).

2.3. SUMO-2/Aβ1-40 cross-linking

SUMO-2 and Aβ1-40 were mixed in equimolar concentrations (10 μM) in PBS and incubated for 10 min before the cross-linking reaction. Proteins were cross-linked with disuccinimidyl dibutyric urea (DSBU, CF Plus Chemicals) and sulfo-NHS diazirine (sSDA, Thermo Fisher Scientific) at a final concentration of 500 μM for 30 min at room temperature. DSBU and sSDA were freshly dissolved in neat dimethyl sulfoxide (DMSO) before addition to the protein solution. DSBU's reaction was quenched using ammonium bicarbonate (ABC) to a final 20 mM concentration. For sSDA, after N-hydroxysuccinimide (NHS) ester labeling, a UV-A irradiation (λ_{max} 360 nm) was performed for 30 s using a home-built LED device. The reaction was then quenched with ABC to a final 20 mM concentration.

2.4. Digestion of cross-linked samples

Cross-linked samples were denatured using 8 M urea in 400 mM ABC and sonicated for 5 min. Samples were reduced with 45 mM dithiotreitol for 30 min at 56 °C and alkylated with 100 mM iodoacetamide for 30 min in the dark. Then, samples were diluted to a final 1 M urea concentration before the addition of the protease. Proteolysis was performed using trypsin overnight or AspN overnight and trypsin for 4 h (1:15 enzyme to protein ratio). Digested samples were quenched using trifluoroacetic acid (TFA) to a pH ~2.

2.5. Mass spectrometry

Proteolyzed samples were subjected to liquid chromatography tandem mass spectrometry (LC-MS) on an UltiMate 3000 RSLC nano-HPLC system (Thermo Fisher Scientific) that was coupled to a trapped ion mobility time of flight (timsTOF) Pro mass spectrometer (Pro MS) equipped with a CaptiveSpray source (Bruker Daltonics). Peptides were

trapped on a C18 column (precolumn Acclaim PepMap 100, 300 μm × 5 mm, 5 μm, 100 Å, Thermo Fisher Scientific) at 50 °C and separated on a self-packed Picofrit (New Objective) nanospray emitter (360 μm o.d. × 75 μm i.d. x 400 mm L, 15 μm Tip i.d.) with C18-stationary phase (3.0 μm, 120 Å, Dr. Maisch GmbH). After trapping, peptides were eluted by a linear 120 min water−acetonitrile (ACN) gradient from 3 % (v/v) to 50 % (v/v). Samples were analyzed using a parallel accumulation serial fragmentation data-dependent acquisition (DDA-PASEF) scheme in two technical replicates. For the timsTOF Pro MS settings, the following parameters were adopted. The mobility-dependent collision energy ramping values were set to 95 eV at an inverse reduced mobility ($1/k_0$) of 1.6 V s/cm^2 and 23 eV at 0.73 V s/cm^2. Collision energies were linearly interpolated between these two $1/k_0$ values and kept constant above or below. No merging of tims scans was performed. Target intensity per individual PASEF precursor was set to 20,000. The scan range was defined between 0.6 and 1.6 V s/cm^2 with a ramp time/accumulation time of 166 ms. 14 PASEF MS/MS scans were triggered per cycle (2.57 s) with a maximum of seven precursors per mobilogram. Precursor ions in an *m/z* range between 100 and 1700 with charge states ≥3+ and ≤8+ were selected for fragmentation. Active exclusion was enabled for 0.4 min (mass width 0.015 Th, $1/k_0$ width 0.015 V s/cm^2). The mass spectrometry proteomics data have been deposited to the ProteomeXchange Consortium via the PRIDE [33] partner repository with the dataset identifier PXD066055.

2.6. Data analysis

Identification of cross-links was performed with MeroX 2.0.1.7 (https://stavrox.com) using a FASTA file containing the sequences of SUMO-2 and Aβ. The following settings were applied: proteolytic cleavage C-terminally at Lys and Arg (trypsin only), up to 3 missed cleavages, or proteolytic cleavage C-terminally at Lys, Arg and N-terminally to Asp, Glu (AspN + trypsin), up to 3 missed cleavages; peptide length: 3 to 30 amino acids; modifications: alkylation of Cys by iodoacetamide (fixed), oxidation of Met (variable). For DSBU, cross-linker specificity: Lys, Ser, Thr, Tyr, N-terminus; search algorithm: RISEUP mode with 3 maximum missing ions, precursor mass accuracy: 15 ppm; fragment ion mass accuracy: 20 ppm; signal-to-noise ratio > 1.5; precursor mass correction enabled, false discovery rate (FDR) cut-off: 5 % (cross-link spectrum match level), and minimum score cut-off: 20. For sSDA, cross-linker specificity: Lys, N-terminus to any amino acid, search algorithm: quadratic mode, precursor mass accuracy: 15 ppm; fragment ion mass accuracy: 20 ppm; signal-to-noise ratio > 1.5; precursor mass correction enabled, FDR cut-off: 5 % (cross-link spectrum match level), and minimum score cut-off: 20.

2.7. Peptide preparation

Aβ1-40 stock solutions for Thioflavin T (ThT) experiments were prepared by dissolving the appropriate amount of protein in PBS 10 mM, 100 mM NaCl, pH 7.4, to reach a final concentration of 250 μM. To prevent the presence of any preformed aggregates, Aβ1-42 was initially dissolved in HFIP at a concentration of 1 mg/mL and then lyophilized overnight. The lyophilized powder was dissolved in 1 mM NaOH for a stock solution with a final concentration of 500 μM. Each stock solution was used immediately after preparation by diluting in the appropriate buffer solution to reach the concentration needed for experiments.

2.8. ThT assay

The kinetics of Aβ1-42 fiber formation were measured by using the ThT assay. Samples were prepared by diluting, in PBS 10 mM, 100 mM NaCl, pH 7.4, a stock solution of Aβ1-42, in the presence or absence of the appropriate amount of Ubiquitin or SUMO-2 to reach the final concentration. ThT was then added to a final concentration of 20 μM. Experiments were carried out in Corning 96-well non-binding surface plates. Time traces were recorded using a Victor Nivo 3S (Revvity, Waltham, MA) plate reader using a 20 nm bandpass filter at 435 nm for excitation and a 30 nm bandpass filter at 480 nm for emission, at 37 °C, shaking the samples for 30 s before each read. All ThT fluorescence curves represent the average of three independent experiments.

2.9. Biolayer interferometry measurements (BLI)

BLI experiments were conducted using high-salt PBS containing 0.02 % Tween 20 and 0.1 % bovine serum albumin (BSA), referred to as KB Buffer (Sartorius, Sartorius Italy S.r.l.). Aβ1-40 or Aβ1-42-biotinylated was prepared at a concentration of 50 μg/ml for use in sensor saturation. The binding assays were performed on an Octet N1 System (Sartorius, Italy S.r.l.) at a controlled temperature of 25 °C. Super Streptavidin Biosensors (SSA, Sartorius, Sartorius Italy S.r.l.) were loaded with biotinylated Aβ peptides at a concentration determined to be optimal (11 μM), selected from a range of 11–400 μM. Sensors were allowed to incubate with the Aβ solution for 300 s dropwise to ensure proper saturation. Biocytin was added at a concentration of 50 μg/ml to quench unbound streptavidin on the sensors. The interaction of amyloid peptides with proteins was analyzed across varying concentrations of 0.15–0.9 mM (Aβ) and 0.01375–0.11 mM (Ubiquitin and SUMO-2), respectively. Binding was assessed over 180 s, followed by a dissociation phase of 200 s. The response intensity (in nanometers) was monitored to evaluate binding kinetics. As a control, the interaction of KB buffer with the biosensor post Aβ saturation was recorded under the same experimental conditions. Wavelength shifts recorded at the 840-second mark (steady-state point) were plotted against corresponding complex concentrations to determine dissociation constants (K_D). The K_D values were estimated by fitting the data to a non-linear regression model based on the one-site specific binding equation: Y=Bmax*X/(K_D+X), where Bmax represents the maximum binding in wavelength shift, and X denotes the concentration of the analyte. The coefficients R^2 and the calculated K_D values for each complex were also calculated. Binding assays were conducted in triplicate, and error bars in the figures represent the standard error of the mean (SEM).

2.10. Circular dichroism (CD)

CD spectra were recorded using a Jasco model 810 spectropolarimeter under a continuous flow of nitrogen, at a scan rate of 50 nm per minute and a resolution of 0.1 nm. The path length was set to 1 cm, covering the 190 to 260 nm range. Spectra were captured as an average of 10 readings. Instrument calibration was conducted using a 0.06 % solution of ammonium camphor sulfonate in water. The concentrations of Aβ1-42, Ubiquitin, and SUMO-2 were freshly prepared at 5–10 μM in a solution of water and PBS (10 mM, pH 7.4, with 1 mM NaCl). CD spectra of the proteins with varying Aβ1-42/protein ratios of 1:1, 1:2, 1:5, and 2:1 were obtained in the same phosphate buffer at 20 °C, using Aβ1-42 stock solution in NaOH. The results are expressed as Δε (molar dichroic coefficient) in M^{-1}.

2.11. SUMOylation reactions in tube tests

In vitro, SUMOylation assays of Ran GTPase-activating protein 1 (RANGAP1) in the presence of monomerized Aβ1-42 were conducted using a SUMOylation assay kit (Abcam #ab139470), following the manufacturer's instructions. Briefly, Aβ1-42 (at concentrations of 2 or 10 μM) was mixed with the reaction buffer and incubated with SUMO-2 at 37 °C for 10 min. Following this, SUMO activating enzyme (E1), Ubiquitin Conjugating enzyme UBC9 (E2), RANGAP1, and ATP were added to achieve a total reaction volume of 30 μL, with a reaction lacking ATP as a negative control. The mixtures were incubated at 37 °C for 60 min, after which reactions were quenched by adding 10 μL of LDS sample buffer (Invitrogen™ 4X Bolt™) and heated to 95 °C for 5 min. The products of the reactions were separated by SDS-polyacrylamide gel

electrophoresis, and the gel was stained using a conventional silver staining protocol. The samples were then transferred onto a nitrocellulose membrane (Amersham™ Protran®). The membranes were blocked with Odyssey blocking buffer (LiCor, Biosciences) for 1 h, followed by an overnight incubation at 4 °C with rabbit anti-SUMO-2,3 (diluted 1:1000, Abcam). After washing the membrane three times for 5 min each with PBST (PBS-0.05 % Tween-20), it was incubated for 40 min with an anti-rabbit IRDye 800–labeled secondary antibody (diluted 1:20000, Li-Cor Biosciences). Membrane visualization was performed with the LI-COR Odyssey IR Imaging System (LI-COR Biosciences, Lincoln). The original images of SDS-PAGE and western blot are reported in Fig. S2 in Supplementary Information.

2.12. Surface plasmon resonance (SPR)

A Sartorius Octet SF3 SPR instrument assessed the kinetic interaction between SUMO-2 and Aβ1-40: covalent Aβ1-40 immobilization was obtained by amine-coupling of the free lysine amino-groups and terminal amines of the peptide with the Carboxy-groups of Carboxymethylated Dextran (CMD) hydrogel, as described elsewhere [34]; The temperature of the autosampler rack and the flow cell was set to 25 °C. The Carboxymethyl Dextran Low Density (CDL) sensor chip was loaded into the Octet SF3 instrument and equilibrated overnight with the running buffer, PBS 10 mM (pH 7.4). Activation of the three channels of the CDL sensor chip was performed immediately prior to Aβ injection through the reaction between EDC (1-ethyl-3-(3-dimethylaminopropyl) carbodiimide) (0.2 M)/NHS (N-hydroxysuccinimide) (0.05 M) solution and the matrix carboxy-groups to achieve reactive succinimide ester groups that can react with the primary amines of Aβ. Lyophilized Aβ1-40 (HFIP-treated) was dissolved in pure DMSO to a final concentration of 1.6 mM and stored in the freezer at −20 °C to obtain a stock Aβ solution. To avoid Aβ aggregation, the injection solutions were prepared immediately before the immobilization step diluting the peptide stock solution in sodium acetate buffer (10 mM, pH 4); the injections were executed at 10 μl/min for 7 min and, in particular, two different concentrations of Aβ were injected in channel one and channel three, 2.31 μM and 11.55 μM respectively, while in channel two (reference channel) only buffer has injected. After the immobilization step, an ethanolamine-HCl 1 M (pH 8.5) solution was injected serially for 7 min at 10 μl/min to deactivate all the residual active sites on the three channels of the CMD sensor chip surface. The overall immobilization rate expressed in Resonace Units (RU) was 77.5 and 590.5 for channels one and three, respectively. Then, the running buffer was changed to PBS with 0.05 % Tween 20, and the system was left to stabilize overnight. A 50 μM solution of SUMO-2 was prepared in PBS with 0.05 % Tween 20 and injected using OneStep® technology [35]. This system utilizes an innovative method based on Taylor dispersion analysis, creating a sigmoidal concentration gradient of the analyte from a single sample vial by dispersing it through a buffer-filled capillary line that flows into the SPR flow cell. From this single injection, kinetic analysis can be conducted to accurately determine the kinetic rate constants and affinity. Two serial injections of SUMO-2 in OneStep® modality, separated by a regeneration step with NaOH 10 mM/NaCl 1 M, were performed at 50 μl/min. The Octet® SPR analysis software carried out the kinetic analysis of the experimental binding curves: the model applied was the "*Two-state*" model, in which a conformational change is involved in the complex formation between SUMO-2 and Aβ. The following equation rules the "*Two state*" fitting model:

$$A + B \underset{k_{d1}}{\overset{k_{a1}}{\rightleftharpoons}} AB \underset{k_{d2}}{\overset{k_{a2}}{\rightleftharpoons}} AB^{*}$$

where A is the analyte, B is the ligand, AB is the initial complex, and AB^{*} is the conformationally changed complex. Moreover, k_{a1} is the association rate constant (single analyte-ligand binding (M^{-1} s^{-1})), k_{d1} is the dissociation rate constant (single analyte-ligand binding (s^{-1})), k_{a2} is the association rate constant for the formation of the conformationally changed complex, k_{d2} is the dissociation rate constant for the formation of the conformationally changed complex, K_D (M) is the equilibrium dissociation constant, R_{max} (RU) is maximum response when all available ligand binding sites are occupied, D_{app} (m^2/s) is the apparent diffusion coefficient, Res SD (RU) is the residual standard deviation of the fitted curves from the experimental curves.

2.13. Preparation of cell lysates

To obtain cell lysates, the neuroblastoma cell line, SH-SY5Y, was grown in Dulbecco's Modified Eagle Medium (DMEM)/F-12 (Gibco, Thermo Fisher) supplemented with 10 % heat-inactivated fetal calf serum (Gibco, Thermo Fisher), 100 mg/ml penicillin and streptomycin (Gibco, Thermo Fisher), and 2 mM L-glutamine (Sigma Aldrich, St. Louis, MO, USA) at 37 °C, 5 % CO_2. Whole cell lysates of untreated cells were prepared by freeze-thawing cycles in water containing 1 mM dithiothreitol (DTT) and a protease and phosphatase inhibitors cocktail (Sigma Aldrich). The lysates were then centrifuged at 10.000 rpm for 20 min, and the supernatants were collected. Protein quantification was determined by the bicinchoninic acid (BCA) protein Assay Kit (Pierce-Thermo Fisher), and an equal amount of proteins were used for mass spectrometry analysis.

2.14. Matrix-assisted laser desorption/ionization time-of-flight (MALDI-TOF) spectrometry

MALDI TOF mass spectra were recorded with an Ultraflextreme MALDI-TOF/TOF mass spectrometer (Bruker Daltonik, Bremen, Germany) operated in linear mode. Ionization was achieved using a nitrogen laser Nd-YAG operating at $\lambda = 337$ nm, pulse width 1–5 ns. The instrument was operated in reflectron or linear midmolecular weight mode, with a mass range set to 2500–30,000 *m/z*. Mass spectra were acquired by averaging 50 shots. The optimized laser intensity remained comparable for all of the analyses. The SA (sinapic acid) matrix was prepared to 10 mg/mL in 50 % ACN and 0.05 % TFA. Standard kits were used to calibrate the mass scale of the MALDI mass spectrometer. 1 μl of matrix solution and 1 μl of sample were deposited on a MALDI matrix target, dried at room temperature, and directly analyzed by MALDI mass spectrometry. The spectra are recorded with FlexControl Software 3.0 (Bruker Daltonik, Bremen, Germany). FlexAnalysis 3.4 (Bruker Daltonik, Bremen, Germany) was used for processing the spectra. Aβ1−42 or SUMO-2 (5 μM), and Aβ1−42/SUMO-2 (1:1 ratio) were solubilized in cell lysate and acquired at room temperature.

2.15. Aβ oligomers preparation

To prepare toxic Aβ1−42 oligomers (oAβ), 1 mg of Aβ1−42 (HFIP-treated) was first dissolved in 5 mM DMSO. A solution of 100 μM Aβ1−42 in ice-cold DMEM-F12 without Phenol Red (Gibco, Thermo Fisher) was prepared and allowed to oligomerize for 48 h at 4 °C under gentle rotation, according to the Lambert protocol with some modifications [36].

2.16. SH-SY5Y cell cultures and MTT assay

The neuroblastoma cell line, SH-SY5Y, was maintained in DMEM-F12 (Gibco, Thermo Fisher) supplemented with 10 % heat-inactivated (HI) fetal calf serum (Gibco, Thermo Fisher), 100 mg/mL penicillin and streptomycin (Gibco, Thermo Fisher), and 2 mM L-glutamine at 37 °C and 5 % CO_2. Two weeks before experiments, 5×10^3 cells were plated on 96-well plates in DMEM-F12 with 5 % HI fetal calf serum. The percentage of serum was gradually decreased until it reached 1 % of the total. All-*trans*-retinoic acid (RA) (Sigma), 5 μM, was used to promote neuronal differentiation, and the medium containing RA was changed every 3 days. Moreover, to evaluate the ability of SUMO-2 to inhibit

toxic Aβ oligomerization, Aβ1-42 monomers were incubated in the presence of SUMO-2 and Ubiquitin at molar ratio of 1:1. After 48 h incubation at 4 °C under gentle rotation, Aβ1-42/SUMO-2 and Aβ1-42/Ubiquitin samples were applied to the differentiated SH-SY5Y cells at the final concentration of 2 μM. The ability of SUMO-2 to interfere with Aβ oligomer toxicity was evaluated by measuring cell viability following 48 hours of treatment. After incubation, cell cultures were exposed to the 3-(4 5-dimethylthiazol-2-yl)-2,5-diphenyltetrazolium bromide (MTT) for 3 h at 37 °C and then lysed with DMSO; the formazan production was evaluated in a multiplate reader (Victor Nivo 3S,

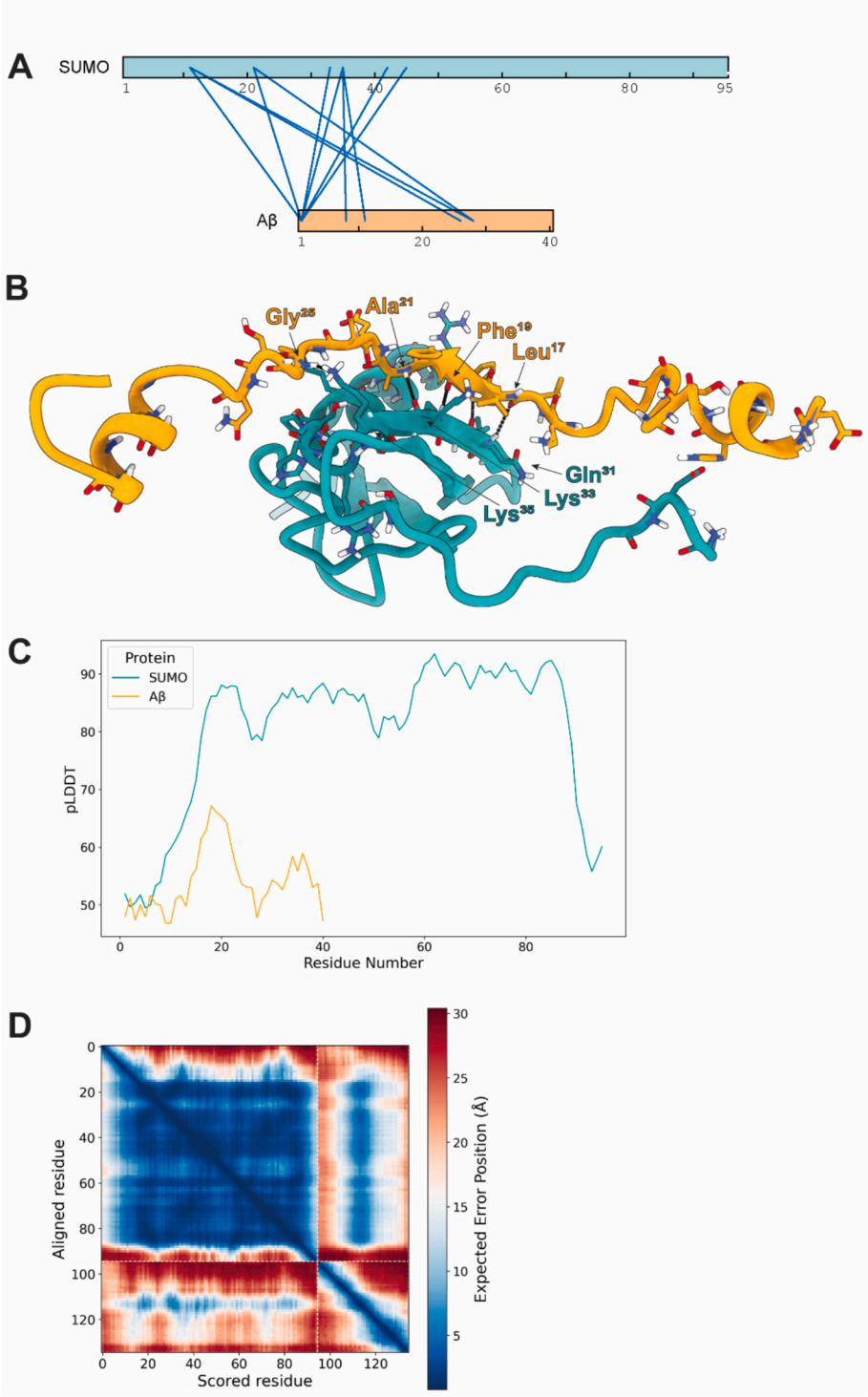

Fig. 1. Investigation of SUMO-2-Aβ1-40 binding interface by XL-MS and AlphaFold 3. A) SUMO-2-Aβ inter-molecular cross-links (in blue) obtained by XL-MS (SUMO-2 is depicted as a green bar, Aβ in orange). Experimental results agree with the interaction surface proposed by AlphaFold3 and indicate Aβ is able to interact with a large portion of SUMO-2. B) AlphaFold3 best predicted SUMO-2-Aβ complex (SUMO-2 represented in green cartoons, Aβ represented in orange). Residues within 5 angstroms (Å) within each protein are shown in the model. C) Residue pLDDT plot for SUMO-2 and Aβ, showing a high local model confidence for SUMO-2 and a poor local model confidence for Aβ (pLDDT >70 for high confidence predictions). D) Predicted aligned error plot for the SUMO-2-Aβ complex predicted by AlphaFold3. Interestingly, AlphaFold3 suggests some regions of contact between the two proteins.

PerkinElmer, Waltham, Massachusetts) through the absorbance at 570 nm.

2.17. HEK 293 cell culture

Cells were cultured in DMEM with 10 % Fetal bovine serum (FBS) and 100 U/ml penicillin-streptomycin and incubated at 37 °C with 5 % CO_2.

2.18. Plasmids and transient transfection

The Aβ-GFP plasmid used in this work was previously described [37]. Plasmid pcDNA3 HA-SUMO-2 WT was a gift from Guy Salvesen (Addgene plasmid # 48967) [38]. Cells were transfected using Lipofectamine™ 3000 (#L3000–015, Invitrogen, Waltham, MA, USA) diluted in serum-free media. The following quantities of total DNA were used: 250 ng/well for the μ-Slide 8 Well imaging chamber.

2.19. Immunofluorescence assays

Medium was removed, cells were washed with room temperature PBS, and cells were fixed in 4 % Paraformaldehyde and 5 % Sucrose in PBS for 10 min. After 3 washes with PBS, cells were permeabilized for 5 min with PBS 0,2 % Triton and blocked for 1 h with PBS 5 % Normal Goat Serum (NGS). Cells were incubated with anti-HA mouse monoclonal antibody (Covance, 1:100 dilution) in blocking buffer for 2 h, followed by 1 h incubation with Alexa secondary anti-mouse antibody. After 3 washes with PBS, cells were incubated with (4′,6-diamidino-2-phenylindole) DAPI (2 μg/mL) for 10′, and left in PBS until confocal microscope acquisition.

2.20. Confocal microscope acquisition

Images were acquired using a confocal A1 system (Nikon, Tokyo, Japan) equipped with a confocal scan unit with 405 nm, 488 nm, 561 nm, and 640 nm laser lines with a scanning sequential mode to avoid bleed-through effects. Images were acquired using a 60× objective over a 20- or 25-μm z axis with a pixel size of 0.21 μm and processed using Imaris software (Bitplane). Three-dimensional acquisitions were displayed as volumes and as x,y single-plane images with z-projections.

3. Results and discussion

3.1. SUMO-2/Aβ contact surfaces determined by cross-linking mass spectrometry (XLMS) and molecular models

To evaluate whether SUMO-2 interacts with Aβ, we initially studied protein/protein interactions in solution using Cross-linking Mass Spectrometry (XL-MS) analysis and AlphaFold AI-based molecular models. We first asked whether chemical cross-linking was capable of capturing the SUMO-2-Aβ1–40 interaction. A 1:1 mixture of SUMO-2 and Aβ1–40 was cross-linked, using cross-linkers of complementary chemistry that could target the whole protein sequences. The cross-linked samples were enzymatically digested and analyzed using nano-LC-MS/MS. This analysis revealed the formation of multiple cross-links between SUMO-2 and Aβ, providing strong evidence of their direct interaction (Fig. 1A). Next, we applied AlphaFold 3 (AF3) to generate a model of SUMO-2 and Aβ (best model shown in Fig. 1B). Aβ supposedly binds to the positively charged surface area of SUMO-2 (Fig. 2A) via a combination of electrostatic and hydrophobic interactions (Fig. 2B). AF3 predicts hydrogen bonds involving residues Gln^{31}, Lys^{35}, Lys^{33} of SUMO-2 and Leu^{17}, Phe^{19}, Ala^{21} and Gly^{25} of Aβ. Furthermore, Aβ residues such as His^{6} and Glu^{22} are in close proximity to residues Asp^{3} and Lys^{42} in SUMO-2, respectively. The AF3 model reveals that SUMO-2 is well-structured upon binding, but Aβ remained intrinsically disordered. The predicted local distance difference test (pLDDT, Fig. 1C) confirmed that SUMO-2 is well-structured, except for its flexible N- and C-terminal tails, while Aβ remains intrinsically disordered, displaying low pLDDT values throughout its sequence. AF3 predicted aligned error plot (Fig. 1D) indicates a low expected positional error at key interaction sites, particularly between amino acids 15–50 in SUMO-2 and 10–25 in Aβ, defining a potential contact surface. Interestingly, our experimental inter-protein cross-links involved Lys residues (namely Lys^{11}, Lys^{35}, Lys^{42}, Lys^{45}), in this exact region of SUMO-2 (Fig. 1D). Altogether, these results defined a putative interaction surface of SUMO-2 as the groove between the second β-strand and the α-helix of the SUMO-2 β-grasp fold.

3.2. Dissociation constants (K_D) of SUMO-2/Aβ complexes

In a previous report, we demonstrated that the amyloid peptide Aβ1-40 binds Ubiquitin with a dissociation constant (K_D = 356 μM) that falls

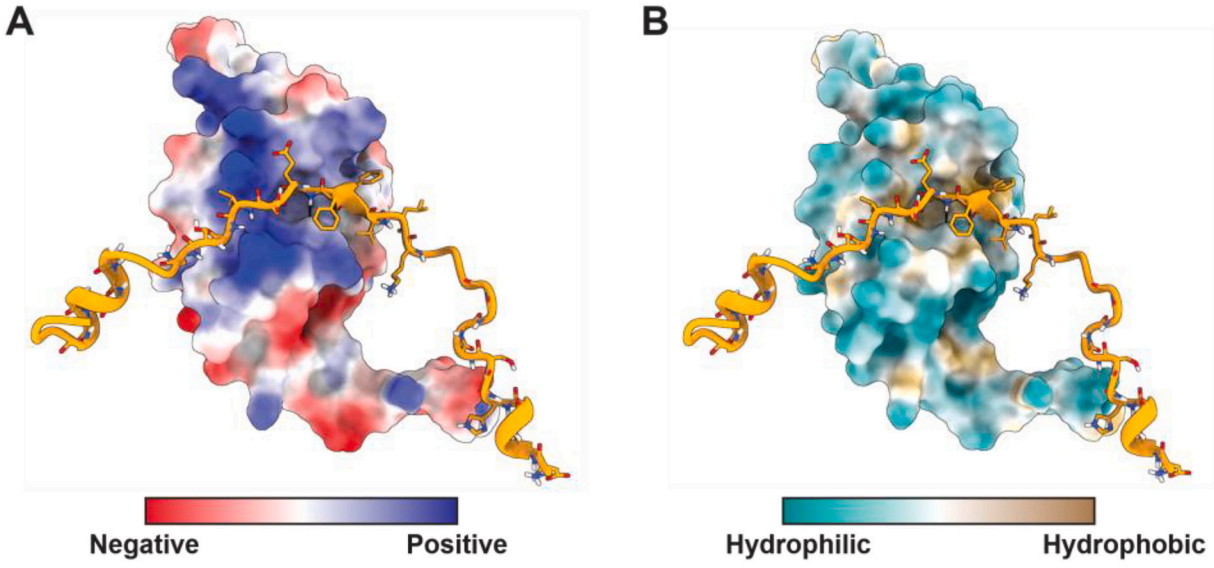

Fig. 2. Interaction surface of SUMO-2 in the AF3 SUMO-2-Aβ complex. A) Aβ is predicted to bind a highly positively charged region of SUMO-2. Aβ is represented in orange cartoons, while SUMO-2 is depicted as surface (color-coded based on its electrostatic potential). B) Aβ-SUMO-2 potentially interacts via a combination of electrostatic and hydrophobic interactions. As in A), Aβ is represented in orange cartoons while SUMO-2 is depicted as surface (color-coded based on its degree of hydrophobicity).

within the range of many Ubiquitin binding partners [39]. In this work, after determining the contact surfaces of the protein/protein complex, we investigated the affinity constants of the Aβ1-40 and Aβ1-42 complex with SUMO-2 by BLI (Fig. 3). In a typical BLI experiment, a sensor chip coated with streptavidin is placed in a sample holder connected to a light source and a detector. The experiment begins by immersing the sensor in a solution containing biotinylated amyloid peptide (loading), allowing the peptide to bind efficiently to the streptavidin coating through a strong biotin-streptavidin interaction (Fig. 3B). Once the loading is complete, the sensor is transferred to a new chamber containing a buffer solution with the protein. As the protein interacts with the immobilized amyloid peptide, real-time measurements of the resulting peptide/protein binding events are captured by the optical system, providing insights into the affinity and kinetics of the interaction. First, we measured the affinity constants of the complex Aβ1-40/Ubiquitin to validate our method. The binding kinetics were analyzed using the Steady State model option of the fitting software. Representative sensograms are reported in Fig. 3A. By employing a 1:1 binding model, we determined that Aβ1-40 has a K_D of 354 μM when interacting with Ubiquitin (Fig. 3 panel C), which aligns with previously published values [39]. After verifying that our method reproduces the literature data, we investigated the potential differences between the binding constants of Ubiquitin with Aβ1-40 and Aβ1-42. Our results indicated that Ubiquitin binds to both Aβ1-40 and Aβ1-42 with comparable affinities, as evidenced by dissociation constants (K_D) of 354 μM and 349 μM, respectively. Next, we investigated the binding kinetics of Aβ peptides to SUMO-2, obtaining K_D values of 137 μM for Aβ1-40 and 104 μM for Aβ1-42 (Table S1 in Supplementary Information). To further validate our results using an alternative experimental method, we performed Aβ1-40 binding studies with SUMO-2 using Surface Plasmon Resonance (SPR). Fig. 3D shows the SPR interaction curves (black) subtracted from the reference channel and the buffer blank injection, while in red, the fitted one is depicted; the green sigmoidal curve is the simulated diffusion profile of SUMO-2, and the fitting parameters are: $Ka_1 = (506 \pm 3\ M^{-1}\ s^{-1})$; $Kd_1 = (0.0777 \pm 0.0004\ s^{-1})$); $Ka_2 = 0.01560 \pm 0.00003\ (RU^{-1}\ s^{-1})$; $Kd_2 = (9.67 \pm 0.02 \times 10^{-4}\ s^{-1})$; $K_D = (154 \pm 1\ \mu M)$; $R_{max} = (57.6 \pm 0.3\ RU)$; $D_{app} = 1.388 \times 10^{-10}$; Res SD value = 0.386. The residual values between the fitted curves and the experimental ones are reported in Fig. 3 panel E. Overall, these results confirm that both Aβ1-40 and Aβ1-42 exhibit similar affinities for SUMO-2, as they do for Ubiquitin. Moreover, they suggest that the affinity of the two peptides for SUMO-2 is significantly greater than that for Ubiquitin.

3.3. SUMO-2 interferes with Aβ1-42 amyloid aggregation

We previously established that amyloid-like aggregation of Aβ1-40 was inhibited upon Ub binding [39]. Similarly, here we aim to evaluate the ability of SUMO-2 to inhibit the aggregation of Aβ1-42, which is considered more toxic than Aβ1-40. To this aim, we performed ThT experiments to compare the ability of Ubiquitin (Fig. 4A), and SUMO-2 (Fig. 4B) to modulate the amyloid growth of Aβ1-42 peptide. Ubiquitin, which is not able to form fibrils by itself (Fig. 4, A purple curve) is known to reduce the fiber formation process of Aβ1-42 [39]. Our measurements fit well with data previously reported, as we observed a progressive decrease of the ThT fluorescence in the plateau region by increasing Ubiquitin concentration (Fig. 4A, green, blue, and red curves respectively) compared with data observed for Aβ1-42 alone (Fig. 4A, black curve). SUMO-2 like Ubiquitin is not able to form fibers (Fig. 4, panel B purple curve), but inhibits Aβ1-42 fiber formation in a concentration-dependent way. Even at sub-stoichiometric concentrations (Fig. 4, panel B, green curve), SUMO-2 increases the lag phase and reduces the total amount of fiber formed. The increase of the lag phase and reduction of ThT maximum fluorescence are even more evident for samples containing higher concentrations of SUMO-2 (Fig. 4B, blue and red curves). Thus, our data suggest a stronger ability of SUMO-2 to interact with Aβ1-42, inhibiting fiber formation or diverting the aggregation pathway towards amorphous aggregation, in agreement with the higher affinity of SUMO-2 for Aβ1-42 compared to Ubiquitin.

3.4. Circular dichroism spectra of Aβ1-42 in the presence of SUMO-2

We investigated whether the interaction between SUMO-2 with Aβ1-42 could mutually induce structural variations. To this aim, we carried out CD spectra of Aβ1-42 and SUMO-2 individually, as well as their respective binary systems at molar ratios of 2:1, 1:1, 1:2, and 1:5. Parallel experiments were carried out with Ubiquitin as a control. The spectra for Ubiquitin and SUMO-2 (5 μM) exhibited negative bands at approximately 207 and 226 nm, indicating as expected, a predominant α-helix conformation (see Fig. 5A and B).

Freshly dissolved 5 μM Aβ1-42 exhibited a random coil structure characterized by a negative band near 200 nm (Fig. 5C). Upon performing repeated measurements on the same sample at 3-, and 7-day intervals, the negative band at 200 nm vanishes while a negative band at 220 nm becomes more pronounced. CD measurements of Aβ1-42 evidenced a conformational change after 3 days, with a shift from a random coil to a β-sheet-rich conformation, consistent with previous studies [36]. In contrast, the structures of Ubiquitin and SUMO-2 showed no significant conformational changes over time. Next, to assess the effects of the interaction with the protein on the conformational preferences of the peptide, we conducted CD experiments on the SUMO-2/Aβ1-42 complexes over time (Fig. 6A and B). The CD spectra of Ubiquitin/Aβ1-42 spectra at a 1:1 ratio showed an increase in the α-helix component compared to Ubiquitin alone. Notably, the SUMO-2/Aβ1-42 system displayed significant profile perturbations in the region around 210 nm. To investigate the effects on peptide conformation, we analyzed the difference spectra between the binary systems and the individual proteins over time (Fig. 6C and D).

The differences in the spectral features of the Aβ1-42/Ubiquitin complex and Aβ1-42/SUMO-2 indicate that in the former case, the Aβ1-42 conformation remains poorly affected by its interaction with Ubiquitin. In contrast, the interaction with SUMO-2 significantly influences the conformational changes in Aβ1-42, resulting in a noticeable decrease in β-sheet content. These results consistently demonstrate that, unlike Ubiquitin, SUMO-2 inhibits the conversion of Aβ1-42 from a random coil to a β-sheet structure. This finding aligns with SUMO-2 higher inhibitory effect on Aβ1-42 aggregation compared to Ubiquitin.

3.5. SUMOylation reactions in tube tests

It is known that exposure to Aβ in primary cortical neurons results in a reduction of SUMOylation [40]. However, despite this biological observation, no hypothesis regarding the underlying molecular mechanisms has been proposed so far.

In a complementary effort to understand the consequences of Aβ/SUMO interactions, we evaluated the effect of Aβ1-42 on SUMOylation reactions by conducting a series of tube test studies using purified SUMO-2, SUMO-conjugating enzymes (UBA2), and a target protein (RANGAP1). Different amounts of the Aβ1-42 peptide (2 and 10 μM) were added to the reaction mixtures, and we assessed SUMOylation activity by monitoring the formation of SUMO-conjugated products using silver staining followed by Western blot analysis (Fig. 7). The positive control for the ATP-dependent SUMOylation reaction involving RANGAP1 shows a band in the 64 kDa region, indicating the formation of the RANGAP1/SUMO-2 conjugate, as previously documented (ab139470 SUMOylation Assay Kit). The absence of this conjugate in the negative control confirms that its formation depends on ATP. Additionally, the same band is significantly diminished in the presence of monomerized Aβ1-42 at 2 and 10 μM concentrations. The results indicate that the Aβ1-42 peptide effectively inhibits SUMOylation, characterized by a significant decrease in the levels of SUMO-conjugated target proteins compared to control reactions without the peptide, even at the lowest concentration (2 μM). These findings demonstrate the peptide's

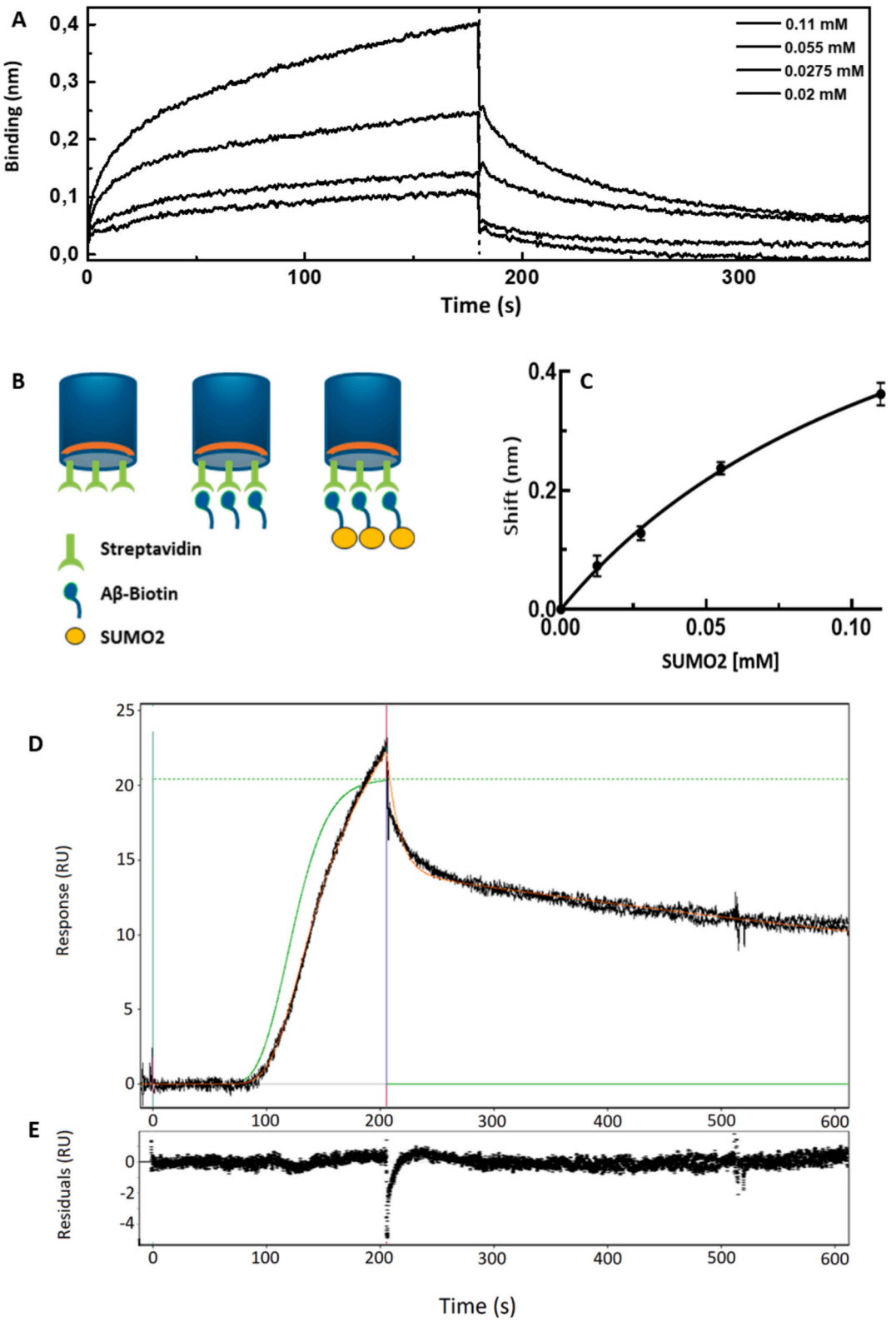

Fig. 3. Dissociation constants (K_D) of the SUMO-2/Aβ1-40 complex were measured by BLI and SPR experiments. A) Raw sensograms obtained from BLI experiments, illustrating the protein/peptide association/dissociation responses over time (concentration range 0.02–0.11 mM). B) Pictogram depicting the strategy employed for the functionalization of the biosensor used in BLI measurements. C) Fitting of the data points derived from the BLI sensograms, enabling the calculation of the affinity constant at steady state. D) Results of surface plasmon resonance (SPR) measurements conducted in parallel with BLI, providing complementary data on K_D of the SUMO-2/Aβ1-40. The black lines refer to the experimental SUMO-2 injection curves (channel three, two experimental repetitions) subtracted from the reference channel two and the buffer blank injection, while the red one is the simulated fitted curve using the "Two State" kinetic model; the green sigmoidal curve represents the simulated diffusion profile of SUMO-2. All the reported results are produced using the OneStep® modality. E) Residual values representing the differences between the experimental SPR curves and the fitted theoretical model, highlighting the accuracy of the data fitting.

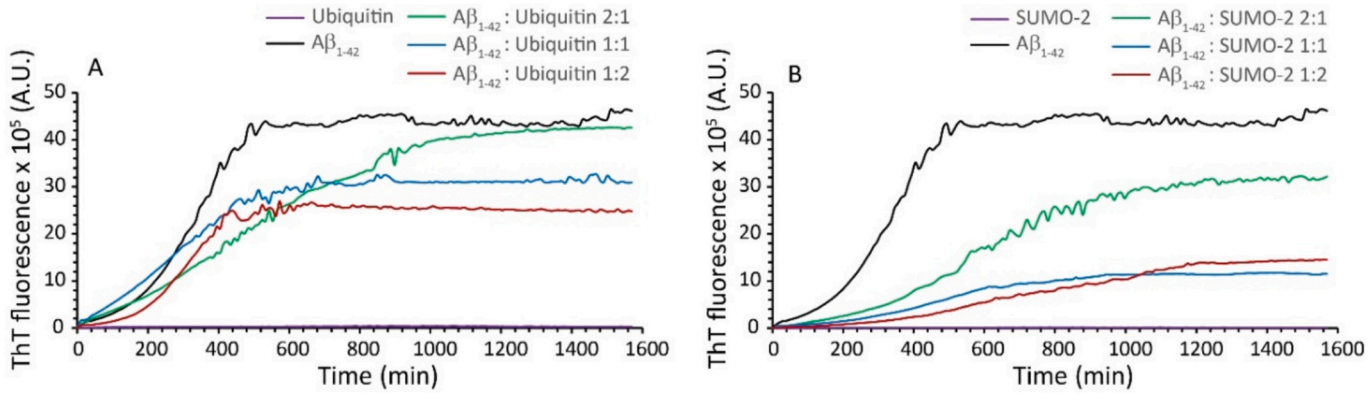

Fig. 4. ThT fluorescence assays. A) Kinetic of fiber formation measured by ThT fluorescence of Ubiquitin 10 μM (purple curve), Aβ1-42 10 μM (black curve), Aβ1-42 10 μM + Ubiquitin 5 μM (green curve), Aβ1-42 10 μM + Ubiquitin 10 μM (blue curve), Aβ1-42 10 μM + Ubiquitin 20 μM (red curve). B) Kinetics of fiber formation measured by ThT fluorescence of SUMO-2 10 μM (purple curve), Aβ1-42 10 μM (black curve), Aβ1-42 10 μM + SUMO-2 5 μM (green curve), Aβ1-42 10 μM + SUMO-2 10 μM (blue curve), Aβ1-42 10 μM + SUMO-2 20 μM (red curve). Experiments were performed in PBS 10 mM, 100 mM NaCl, pH 7.4 at 25 °C. All traces are the average of 3 independent experiments.

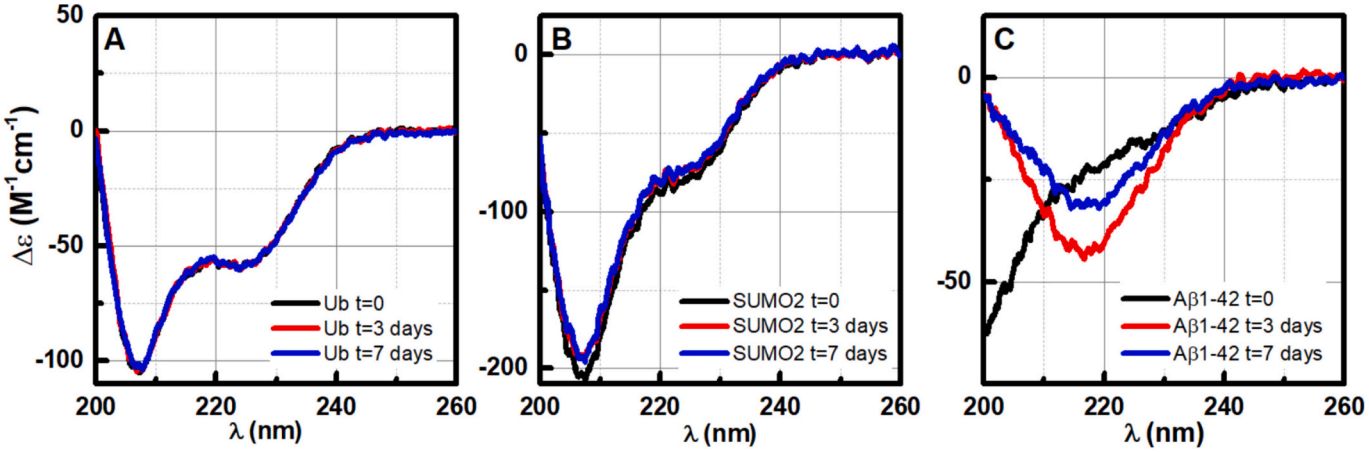

Fig. 5. UV-CD spectra over time of: A) Ubiquitin, B) SUMO-2 and C) Aβ1-42 in PBS 10 mM, 1 mM NaCl, pH 7.4.

capability to impact the dynamics of SUMOylation and open avenues for further exploration into its potential regulatory roles in cellular signaling processes.

3.6. *Aβ1-42 competitively interacts with SUMO-2 in complex biological mixtures*

Experiments conducted in tube tests have shown that Aβ peptides bind to SUMO-2 with a binding affinity similar to ubiquitin. To strengthen the biological significance of our findings, the next step was to verify whether Aβ can competitively bind to SUMO-2 in the presence of the complete pool of cellular SUMO-2 binding partners. To achieve this, we examined the interaction between SUMO-2 and the Aβ peptide using whole cell extracts from SH-SY5Y cells. MALDI-MS is an effective technique for analyzing protein-protein interactions in complex biological mixtures. In this study, we utilized MALDI-MS to demonstrate that Aβ retains its ability to bind SUMO-2 even when all native cytosolic SUMO-2 binding partners are present. We performed MALDI-MS measurements to identify the potential presence of soluble Aβ oligomeric structures and to investigate their interaction with SUMO-2 protein (see Table S2). In particular, we wanted to test whether an eventual adduct could also exist in the presence of lysate, opportunely diluted, and of its components. In Fig. 8 the spectrum of Aβ1−42 reported in black, shows a major peak for the Aβ1−42 monomer ($m/z = 4514$) and lower signals for its dimer (m/z = 9028), trimer (m/z = 13,543) and tetramer (m/z = 18,056). The SUMO-2 spectrum (reported in blue) indicates a major peak for the SUMO-2 sodium adduct species at m/z = 11,002 (SUMO-2 + 4Na + K) and the minor peak of its dimer at m/z = 21,996 (2SUMO-2 + 6Na + 3 K). Interestingly, in addition to the peaks relating to the two proteins, the spectrum of the Aβ/SUMO-2 system (shown in red) highlights the presence of an additional small peak at m/z = 15,517. The latter confirms the interaction between the protein and Aβ1−42, forming an equimolar noncovalent adduct.

3.7. *SUMO-2 does not directly interfere with toxic Aβ1-42 oligomerization*

The ThT (Fig. 4) spectra conducted in this study suggest that SUMO-2 may inhibit the amyloid-like aggregation of Aβ1-42 peptides. To investigate whether the non-covalent interaction could also affect a typical process involved in AD progression, we tested the ability of SUMO-2 to interfere with the formation of oligomers, which are known to be responsible for Aβ1-42 toxicity. To better analyze the effect of SUMO-2 on the oligomerization process, we co-incubated freshly prepared monomeric Aβ1-42 and SUMO-2 protein at a molar ratio of 1:1 for 48 h at 4 °C in a DMEM-F12 medium without phenol Red, according to a well-established protocol [36]. Samples with the same concentration of Ubiquitin have been used as a control.

After incubation, all samples have been tested on human differentiated cells, SH-SY5Y, in order to assess whether SUMO-2 could interfere

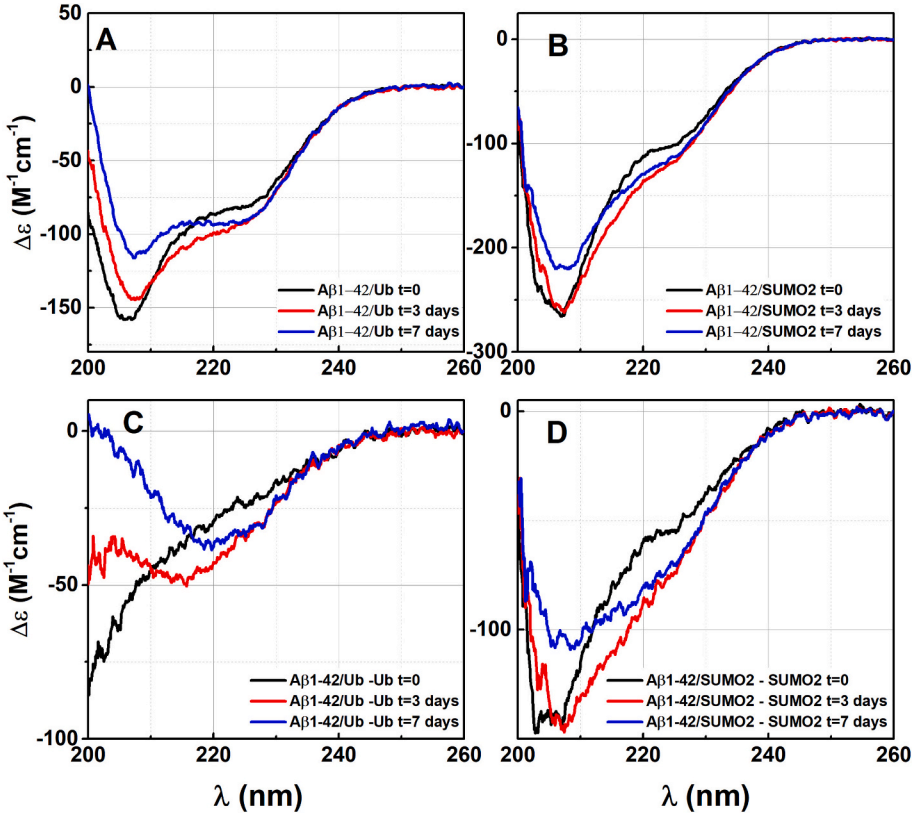

Fig. 6. CD Spectra of binary systems A) Aβ1-42/Ub; B) Aβ1-42/SUMO-2 in PBS 10 mM 1 mM NaCl pH 7.4 are shown in the wavelength (λ) range of 200–260 nm. The difference spectra obtained by subtracting the corresponding Ubiquitin spectrum from the Aβ1-42/Ubiquitin binary system are shown in C. Similarly, for SUMO-2, the difference spectra are reported in D. All CD spectra are collected over a period of a week (t = 0, black; t = 3 days, red; t = 7, blue).

with the aggregation of Aβ1-42, also under oligomerization conditions. Cells were exposed for 48 h to oligomers at a final concentration of 2 μM, either in the presence or in the absence of SUMO-2/Ubiquitin, whose ability to reduce Aβ1-42 toxicity was assessed by the 3-(4 5-dimethylthiazol-2-yl)-2,5-diphenyltetrazolium bromide (MTT) assay.

As expected, cells exposed to oligomers derived from the aggregation of Aβ peptide alone, exhibited a reduction in cell viability of approximately 30 %. Neither SUMO-2 nor Ubiquitin was able to mitigate the toxicity of oAβ, revealing that SUMO-2 does not interfere with Aβ self-assembly under oligomeric-driven conditions (Fig. 9).

3.8. Co-localization of SUMO-2 and Aβ1-42 aggregates in HEK293 cells co-expressing HA-SUMO-2 and Aβ1-42-GFP

We performed immunofluorescent labeling and confocal microscopy analysis 24 h after transfection to confirm the biological significance of our investigations and validate the potential interaction between SUMO-2 and Aβ1-42 within living cells. As shown in Fig. 10, HEK293 cells that express Aβ1-42 alone display large aggregates in both the nucleus and cytoplasm. These significant Aβ aggregates result in nuclear fragmentation, potentially leading to cell death. Conversely, cells that co-express Aβ1-42 and SUMO-2 show colocalization of the two proteins in distinct granules found in both the cytoplasm and nucleus, suggesting a possible interaction between SUMO-2 and Aβ1-42 in living cells.

Further insights are provided by Fig. 11, which illustrates two distinct scenarios of Aβ1-42 and SUMO-2 expression.

The cell on the left shows high levels of SUMO-2, resulting in a diffuse distribution of Aβ1-42 throughout the cytoplasm. Conversely, the cell on the right exhibits lower levels of SUMO-2, corresponding to numerous visible Aβ1-42 aggregates. This variability in SUMO-2 expression appears to influence the aggregation state of Aβ1-42, indicating that SUMO-2 may modulate the localization and behavior of Aβ1-42 within the cell. Overall, these findings underscore the colocalization of SUMO-2 and Aβ1-42 in living cells, as observed through three-dimensional imaging and z-projections.

4. Discussion

Although SUMO-2 signaling and Aβ peptides accumulation are known to play a role in AD, their non-covalent interactions have received little attention. To address this issue, we measured the dissociation constants of the SUMO-2/Aβ peptide complexes and characterized their contact surfaces. The interaction between Aβ and SUMO-2 is driven by an H-bond network involving SUMO-2 residues Gln^{31}, Lys^{35}, Lys^{33}, and Aβ residues Leu^{17}, Phe^{19}, Ala^{21}, and Gly^{25}. Aβ residues such as His^{6} and Glu^{22} are also in close proximity to residues Asp^{3} and Lys^{42} in SUMO-2, respectively, but also involve Lys residues (namely Lys^{11}, Lys^{35}, Lys^{42}, Lys^{45}). Altogether, these results defined a putative interaction surface of SUMO as the groove between the second β-strand and the α-helix of the SUMO β-grasp fold. SUMO-2 is normally conjugated to a lysine (K) in target proteins that is frequently located in the SUMOylation consensus motif ψKxE (ψ is a large hydrophobic residue) or in the inverted motif [E/D]x [41,42]. Lys^{11} in SUMO-2 is situated in a SUMOylation consensus motif and Lys^{11}-linked SUMO-2 is therefore the most frequently found SUMO polymer, constituting ~90 % of the SUMO polymers [43,44]. On the other hand, non-covalent SUMO interactions are critical to allow SUMO recognition. Proteins that can read SUMO modification usually contain one or multiple SUMO interacting motifs (SIMs) to enable their interaction with SUMOylated targets [45]. SIMs consist of short stretches of the large hydrophobic residues leucine, isoleucine or valine, frequently flanked by acidic residues [42]. These structural analyses indicate that the interaction surfaces with Aβ peptides, particularly the hydrophobic and charged residues, could overlap with the interaction interface of SUMO-2 with target proteins. These

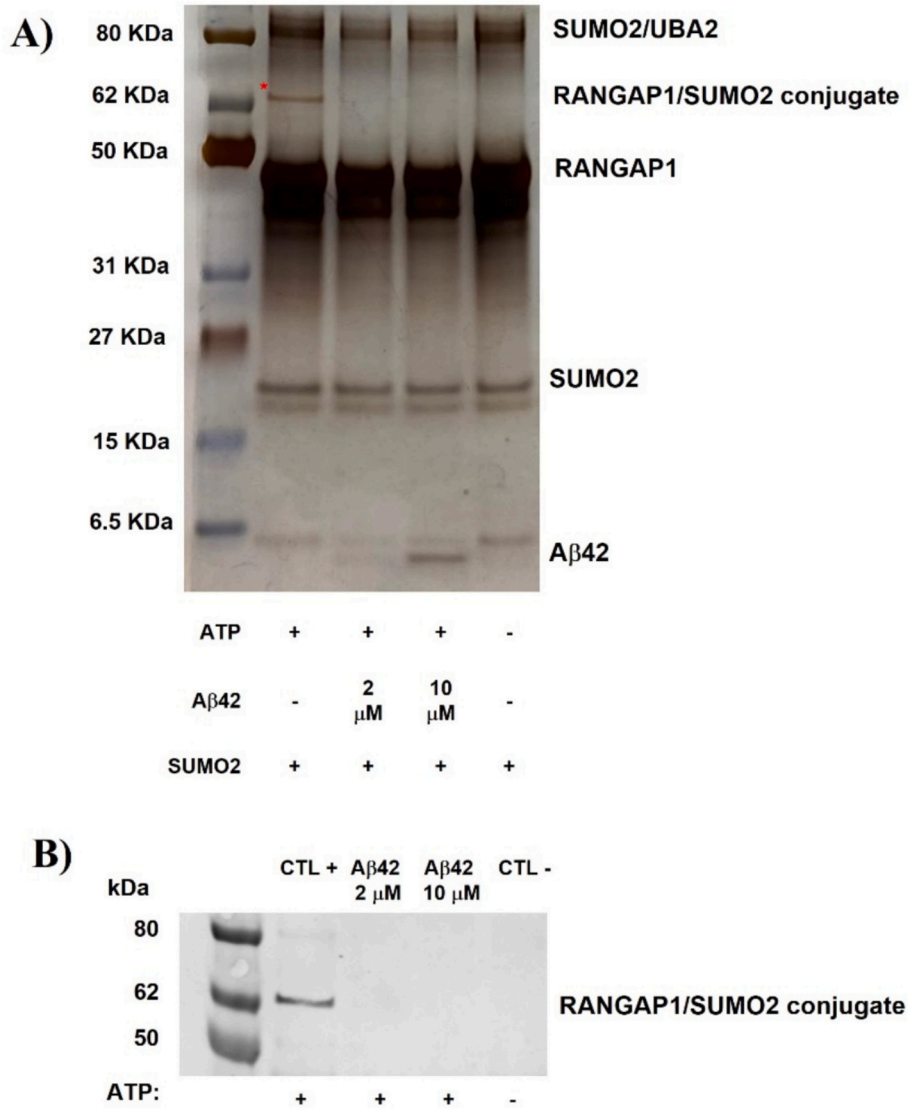

Fig. 7. A) Representative silver staining of gradient SDS-PAGE gel. B) Representative western blot of RANGAP1/SUMO-2 conjugate.

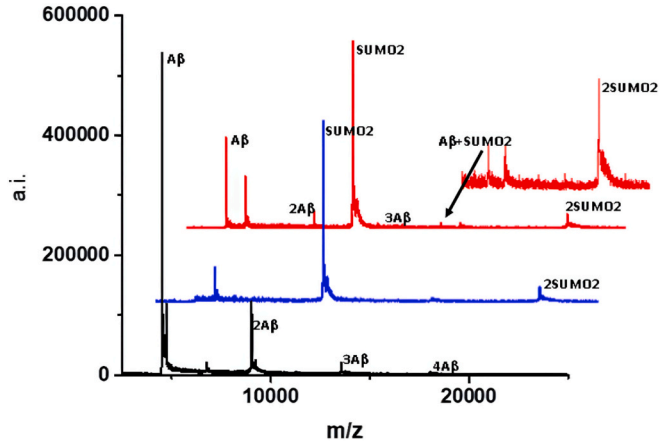

Fig. 8. MALDI-TOF spectra of Aβ peptide alone (black); SUMO-2 protein alone (blue) and Aβ + SUMO-2 complex (red). The inset shows an enlarged view of the Aβ/SUMO-2 adduct peak.

observations reconcile with our experimental data, which showed that when attempting to reproduce SUMOylation in tube tests, the presence of the Aβ peptide completely inhibits the reaction.

Our structural models indicate that specific residues in Aβ may form hydrogen bonds and hydrophobic interactions with SUMO-2. For instance, the aggregation-prone regions of Aβ possess a significant density of hydrophobic side chains such as phenylalanine and leucine, which are known to interact with the hydrophobic pockets of proteins. Further experimental data obtained through CD measurements have highlighted that the interaction with SUMO-2 induces a delay in the conformational transitions from random coil to β-sheet of the Aβ peptide. These data reconcile well with the observations mentioned above. It should also be noted that ThT fluorescence studies have shown that, in accordance with CD data, the aggregation process of the Aβ in the presence of SUMO-2 results inhibited. Given the possible implications of these findings in AD mechanisms, it is crucial to carefully evaluate the biological relevance of these interactions. Accordingly, we measured the dissociation constants of Aβ peptides with SUMO-2. For ubiquitin, the dissociation constants of several binding partners are well-documented, ranging from 2 to 500 μM [46]. In contrast, there is limited data on the dissociation constants of SUMO-2 with its potential partners, raising questions about the hypothesis of a direct interaction between SUMO-2

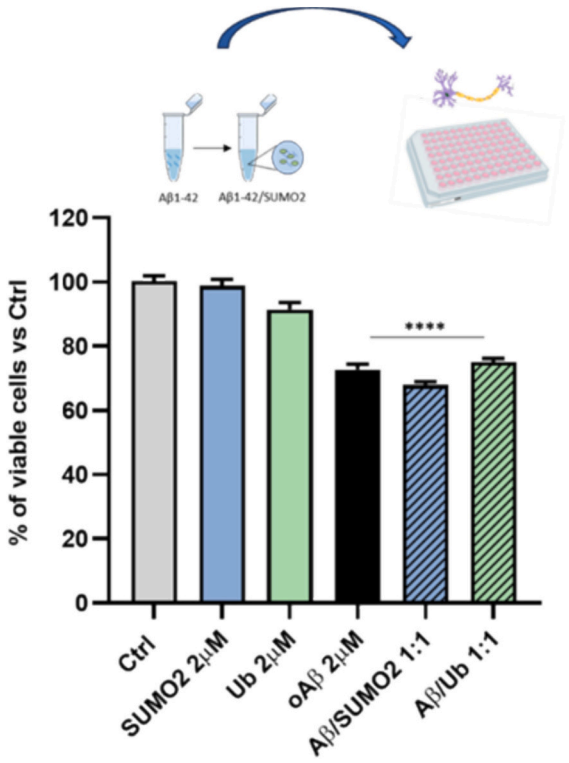

Fig. 9. MTT assay of fully differentiated SH-SY5Y cells treated for 48 h with Aβ1-42 oligomers prepared in the presence or absence of SUMO-2/Ubiquitin at the molar ratio of 1:1. Samples were incubated at 4 °C under gentle rotation for 48 h. Bars represent means ± SEM of three independent experiments with n = 4 each. ****P < 0.0001 vs Ctrl by one-way ANOVA + Tukey test.

and Aβ in a cellular context.

Our results show that Aβ1-40 and Aβ1-42 have dissociation constants of 354 μM and 349 μM, respectively, when binding to Ubiquitin, and 137 μM and 104 μM when interacting with SUMO-2. This suggests that both Aβ amyloid peptides may be classified as Ubiquitin binding proteins, but may have a stronger preference for SUMO-2 because of its lower dissociation constants. However, it is also important to consider the relative concentrations of these proteins within cells. For instance, SUMO-2 is one of the top 20 most abundant proteins, with approximately 8.8 million copies per cell [35]. However, Ubiquitin is slightly more abundant, with around 14.5 million copies per cell [47]. Therefore, even though SUMO-2 demonstrates a stronger binding affinity for Aβ peptides than Ubiquitin, the overall concentrations of these proteins may influence the relative amounts of the two protein-peptide complexes. Nevertheless, as SUMO-2 is primarily localized in the nucleus [48] whereas a Ubiquitin is dispersed throughout the entire cell, Ubiquitin may modestly compete with SUMO-2 for target proteins within the nucleus. For these reasons, the interaction between SUMO-2 and Aβ peptides are biologically relevant. To further support this hypothesis, we incubated Aβ peptides and SUMO-2 with cell extracts and used MALDI-MS to detect SUMO-2/Aβ1-42 adducts. This experiment showed that even with all possible SUMO binding partners present, the interaction between SUMO-2 and Aβ still occurs. This result confirms that this interaction is important in a biological context.

Noteworthy, the nuclear co-localization of SUMO-2 and Aβ constructs, transiently transfected in HEK293 cells, confirmed that the non-covalent interaction observed in vitro does indeed occur in the cellular environment. The role of SUMO-2 in alleviating the toxic effects of Aβ is becoming increasingly evident in the literature. Overexpression of human SUMO-2 has been proven to prevent synaptic dysfunction and cognitive impairments caused by Aβ oligomers, suggesting an interplay between the protein and the aberrant process of toxic aggregate formation [32]. Based on this evidence and in light of the data obtained in this work, we finally investigated the effect of SUMO-2 on Aβ self-assembly under oligomeric-driven conditions. As demonstrated by the viability assay, the presence of SUMO-2 did not interfere with the formation of toxic species, suggesting that its neuroprotection and cognitive restoration activity are not dependent on a direct effect on Aβ oligomerization.

In conclusion, the contact surfaces between Aβ peptides and SUMO-2 provide a foundation for understanding how amyloid peptides may inhibit SUMOylation reactions. Through competitive binding, conformational destabilization, and functional alteration of SUMO-2, we propose that amyloid peptides could exacerbate cellular dysfunction in neurodegenerative diseases. These hypotheses warrant further investigation through experimental assays, including binding studies with different in vivo models, to confirm the direct impact of amyloid peptides on SUMOylation and their broader implications in neurodegeneration.

CRediT authorship contribution statement

Valeria Ciaffaglione: Visualization, Methodology, Investigation, Formal analysis, Data curation. **Giulia Grasso:** Writing – review & editing, Writing – original draft, Validation, Methodology, Investigation, Data curation, Conceptualization. **Valeria Lanza:** Writing – review & editing, Validation, Methodology, Investigation, Data curation, Conceptualization. **Michele Francesco Maria Sciacca:** Writing – review & editing, Writing – original draft, Visualization, Validation, Methodology, Investigation, Data curation, Conceptualization. **Stefania Zimbone:** Writing – review & editing, Writing – original draft, Validation, Methodology, Investigation, Data curation, Conceptualization. **Maria Laura Giuffrida:** Writing – review & editing, Writing – original draft, Validation, Methodology, Investigation, Data curation, Conceptualization. **Claudio Iacobucci:** Writing – review & editing, Writing – original draft, Visualization, Validation, Methodology, Investigation, Data curation, Conceptualization. **Alessio Di Ianni:** Writing – review & editing, Writing – original draft, Visualization, Validation, Methodology, Investigation, Data curation, Conceptualization. **Damiano Calcagno:** Writing – review & editing, Writing – original draft, Visualization, Validation, Methodology, Investigation, Data curation, Conceptualization. **Giuseppe Grasso:** Writing – review & editing, Writing – original draft, Visualization, Validation, Resources, Methodology, Funding acquisition, Data curation. **Andrea Alloni:** Visualization, Validation, Methodology, Investigation, Data curation. **Franca Orsini:** Visualization, Validation, Methodology, Investigation, Data curation. **Paul Fraser:** Writing – review & editing, Writing – original draft, Resources, Methodology, Conceptualization. **Luana Fioriti:** Writing – review & editing, Writing – original draft, Visualization, Validation, Resources, Methodology, Data curation, Conceptualization. **Danilo Milardi:** Writing – review & editing, Writing – original draft, Visualization, Resources, Project administration, Funding acquisition, Conceptualization.

Funding

This study was financially supported by the Ministero dell'Università e della Ricerca: "Funded by European Union - Next Generation EU, Mission 4 Component C2, CUP: B53D23025960001-PRIN PNRR grant no. P2022YRPHS" and "Funded by European Union - Next Generation EU, Mission 4 Component C2, CUP: B53D23016440006-PRIN grant no. 2022PAAYZE". We thank the research project "Potentiating the Italian Capacity for Structural Biology Services in Instruct Eric" (Acronym: ITACA.SB, project no. IR0000009) within the call MUR D.D. 0003264 dated 28/12/2021 PNRR M4/C2/L3.1.1, funded by the European Union NextGenerationEU. The authors acknowledge the Italian Ministry of Health and Fondazione Roma for their support. Financial support was also provided by the Canadian Institutes of Health Research (PJT-

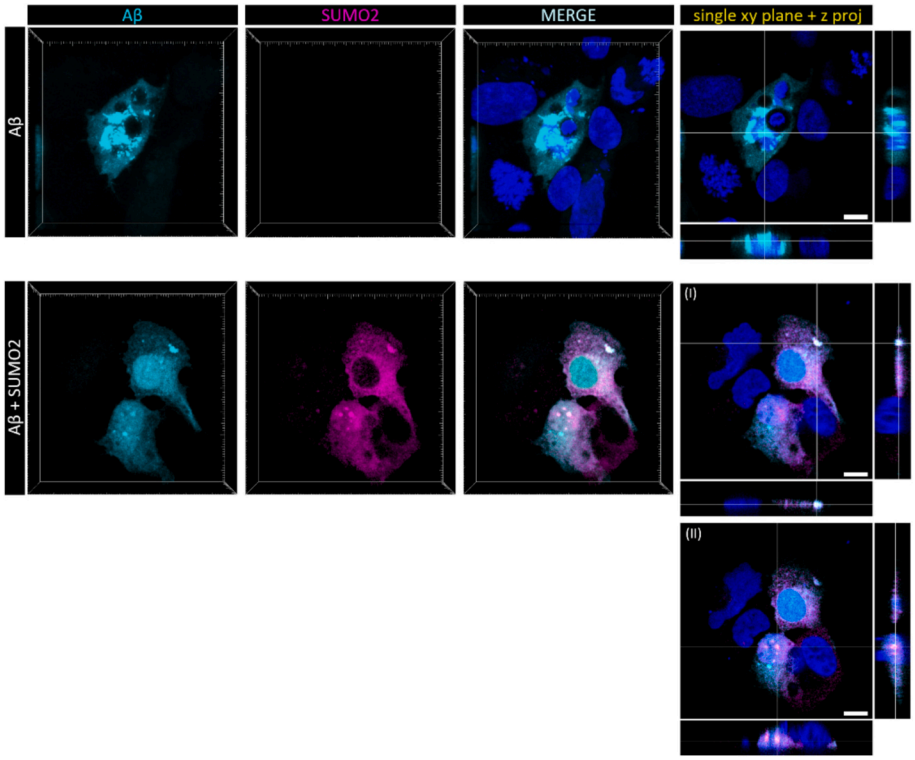

Fig. 10. SUMO-2 colocalizes with Aβ1-42 in transfected cells. Representative images of HEK293 cells expressing Aβ (cyan) alone or in combination with SUMO-2 (magenta) 24 h after transfection. The upper panels show an Aβ1-42-expressing cell, full of large aggregates in both the nucleus and the cytoplasm. The lower panels show cells expressing both Aβ1-42 and SUMO-2, which colocalize in granules, suggesting an association between the two proteins in the cellular environment. These granules were found in both the cytoplasm (I) and the nucleus (II). Three-dimensional images were acquired using a confocal microscope and displayed as volumes, as well as x,y single-plane images with z-projections (right panels). Scale bar: 10 μm.

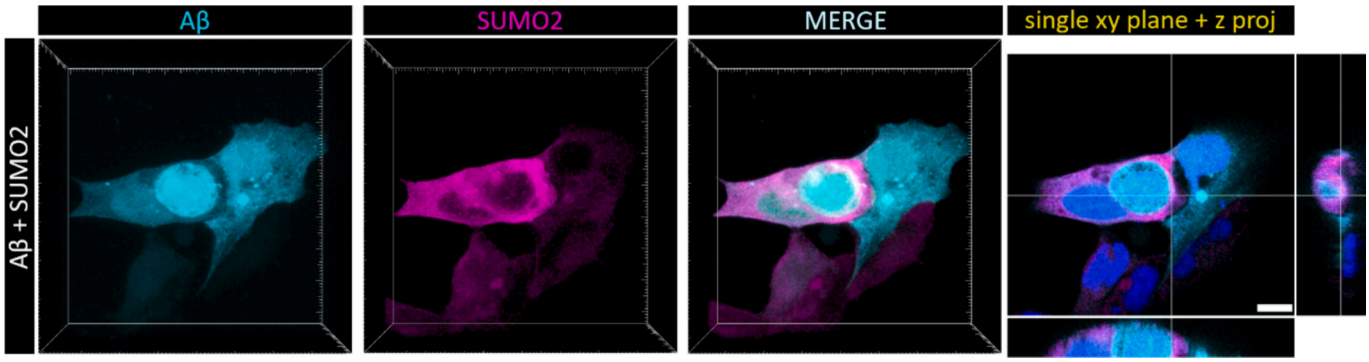

Fig. 11. SUMO-2 colocalizes with Aβ1-42 in transfected cells. Representative images of HEK293 cells expressing Aβ1-42 (cyan) in combination with SUMO-2 (magenta) 24 h after transfection. In this image, the cell on the left expresses high levels of SUMO-2, resulting in a diffuse Aβ1-42 signal across the cell. In contrast, the cell on the right has low SUMO-2 expression, with many visible Aβ aggregates. Three-dimensional image was acquired using a confocal microscope and displayed as volumes, as well as x,y single-plane images with z-projections (right panels). Scale bar: 10 μm.

173497 to PF).

Declaration of competing interest

The authors declare that they have no known competing financial interests or personal relationships that could have appeared to influence the work reported in this paper.

Data availability

Data will be made available on request.

Appendix A. Supplementary data

Supplementary data to this article can be found online at https://doi.org/10.1016/j.ijbiomac.2025.146632.

References

[1] Ö.Ö. Tozlu, H. Türkez, U. Okkay, O. Ceylan, C. Bayram, A. Hacımüftüoğlu, A. Mardinoğlu, Assessment of the neuroprotective potential of d-cycloserine and l-serine in aluminum chloride-induced experimental models of Alzheimer's disease: in vivo and in vitro studies, Front. Nutr. 9 (2022) 981889.
[2] G.G. Glenner, C.W. Wong, Alzheimer's disease: initial report of the purification and characterization of a novel cerebrovascular amyloid protein, Biochem. Biophys. Res. Commun. 120 (1984) 885–890.

[3] J. Kang, H.G. Lemaire, A. Unterbeck, J.M. Salbaum, C.L. Masters, K.H. Grzeschik, G. Multhaup, K. Beyreuther, B. Müller-Hill, The precursor of Alzheimer's disease amyloid A4 protein resembles a cell-surface receptor, Nature 325 (1987) 733–736, https://doi.org/10.1038/325733a0.

[4] C.L. Masters, G. Simms, N.A. Weinman, G. Multhaup, B.L. McDonald, K. Beyreuther, Amyloid plaque core protein in Alzheimer disease and Down syndrome, Proc. Natl. Acad. Sci. USA 82 (1985) 4245–4249.

[5] D.J. Selkoe, Normal and abnormal biology of the β-amyloid precursor protein, Annu. Rev. Neurosci. 17 (1994) 489–517, https://doi.org/10.1146/annurev.ne.17.030194.002421.

[6] I.W. Hamley, The amyloid beta peptide: a chemist's perspective. Role in Alzheimer's and fibrillization, Chem. Rev. 112 (2012) 5147–5192, https://doi.org/10.1021/cr3000994.

[7] S. Oddo, A. Caccamo, I.F. Smith, K.N. Green, F.M. LaFerla, A dynamic relationship between intracellular and extracellular pools of Aβ, Am. J. Pathol. 168 (2006) 184–194.

[8] C. Barucker, A. Harmeier, J. Weiske, B. Fauler, K.F. Albring, S. Prokop, P. Hildebrand, R. Lurz, F.L. Heppner, O. Huber, Nuclear translocation uncovers the amyloid peptide Aβ42 as a regulator of gene transcription, J. Biol. Chem. 289 (2014) 20182–20191.

[9] J.T. Jarrett, E.P. Berger, P.T. Lansbury, The carboxy terminus of the β amyloid protein is critical for the seeding of amyloid formation: implications for the pathogenesis of Alzheimer's disease, Biochemistry 32 (1993) 4693–4697, https://doi.org/10.1021/bi00069a001.

[10] T. Qiu, Q. Liu, Y.-X. Chen, Y.-F. Zhao, Y.-M. Li, Aβ42 and Aβ40: similarities and differences, J. Pept. Sci. 21 (2015) 522–529.

[11] S. Jevtic, J. Provias, The amyloid precursor protein: more than just amyloid-beta, J. Neurol. Exp. Neurosci. 5 (2019) 1–11.

[12] G.D. Rabinovici, W.J. Jagust, Amyloid imaging in aging and dementia: testing the amyloid hypothesis in vivo, Behav. Neurol. 21 (2009) 117–128.

[13] G. Grasso, M.L. Giuffrida, E. Rizzarelli, Metallostasis and amyloid β-degrading enzymes, Metallomics 4 (2012) 937–949, https://doi.org/10.1039/c2mt20105d.

[14] R. Dhapola, S.K. Beura, P. Sharma, S.K. Singh, D. HariKrishnaReddy, Oxidative stress in Alzheimer's disease: current knowledge of signaling pathways and therapeutics, Mol. Biol. Rep. 51 (2024) 48, https://doi.org/10.1007/s11033-023-09021-z.

[15] J. Sun, J. Yang, K. Whitman, C. Zhu, D.H. Cribbs, R.J. Boado, W.M. Pardridge, R. K. Sumbria, Hematologic safety of chronic brain-penetrating erythropoietin dosing in APP/PS1 mice, Alzheimers Dement. Transl. Res. Clin. Interv. 5 (2019) 627–636.

[16] S. Kumar, S. Kumar, H. Ram, Anti-aggregation property of allicin by *in vitro* and molecular docking studies, J. Exp. Neurosci. 13 (2019) 117906951986618, https://doi.org/10.1177/1179069519866185.

[17] L. Gong, D.W.-C. Li, Sumoylation in ocular development and pathology, Curr. Mol. Med. 10 (2010) 794–801, https://doi.org/10.2174/156652410793937769.

[18] S. Accossato, F. Kessler, V. Shanmugabalaji, Sumoylation contributes to proteostasis of the chloroplast protein import receptor TOC159 during early development, Elife 9 (2020) e60968.

[19] U. Sahin, P. Lapaquette, A. Andrieux, G. Faure, A. Dejean, Sumoylation of human argonaute 2 at lysine-402 regulates its stability, PLoS One 9 (2014) e102957.

[20] Q. Zhao, Y. Xie, Y. Zheng, S. Jiang, W. Liu, W. Mu, Z. Liu, Y. Zhao, Y. Xue, J. Ren, GPS-SUMO: a tool for the prediction of sumoylation sites and SUMO-interaction motifs, Nucleic Acids Res. 42 (2014) W325–W330.

[21] G. Grasso, V. Lanza, G. Malgieri, R. Fattorusso, A. Pietropaolo, E. Rizzarelli, D. Milardi, The insulin degrading enzyme activates ubiquitin and promotes the formation of K48 and K63 diubiquitin, Chem. Commun. 51 (2015) 15724–15727, https://doi.org/10.1039/C5CC06786C.

[22] R. Geiss-Friedlander, F. Melchior, Concepts in sumoylation: a decade on, Nat. Rev. Mol. Cell Biol. 8 (2007) 947–956.

[23] L. Colnaghi, L. Russo, C. Natale, E. Restelli, A. Cagnotto, M. Salmona, R. Chiesa, L. Fioriti, Super resolution microscopy of SUMO proteins in neurons, Front. Cell. Neurosci. 13 (2019), https://doi.org/10.3389/fncel.2019.00486.

[24] J. Lin, Y. Ai, H. Zhou, Y. Lv, M. Wang, J. Xu, C. Yu, H. Zhang, M. Wang, UL36 encoded by Marek's disease virus exhibits linkage-specific deubiquitinase activity, Int. J. Mol. Sci. 21 (2020) 1783.

[25] C. Conte, E.R. Griffis, I. Hickson, A.B. Perez-Oliva, USP45 and Spindly are part of the same complex implicated in cell migration, Sci. Rep. 8 (2018) 14375.

[26] L. Wang, C. Wansleeben, S. Zhao, P. Miao, W. Paschen, W. Yang, SUMO2 is essential while SUMO3 is dispensable for mouse embryonic development, EMBO Rep. 15 (2014) 878–885, https://doi.org/10.15252/embr.201438534.

[27] G. Gill, SUMO and ubiquitin in the nucleus: different functions, similar mechanisms? Genes Dev. 18 (2004) 2046–2059.

[28] J.D. Bernstock, D.G. Ye, D. Estevez, G. Chagoya, Y.-C. Wang, F. Gessler, J. M. Hallenbeck, W. Yang, The role of sumoylation and ubiquitination in brain ischaemia: critical concepts and clinical implications, Curr. Issues Mol. Biol. 35 (2020) 127–144.

[29] L. Lee, E. Dale, A. Staniszewski, H. Zhang, F. Saeed, M. Sakurai, M. Fa', I. Orozco, F. Michelassi, N. Akpan, Regulation of synaptic plasticity and cognition by SUMO in normal physiology and Alzheimer's disease, Sci. Rep. 4 (2014) 7190.

[30] L. Lee, E. Dale, A. Staniszewski, H. Zhang, F. Saeed, M. Sakurai, I. Orozco, F. Michelassi, N. Akpan, H. Lehrer, Corrigendum: regulation of synaptic plasticity and cognition by SUMO in normal physiology and Alzheimer's disease, Sci. Rep. 5 (2015) 11782.

[31] Y. Li, H. Wang, S. Wang, D. Quon, Y.-W. Liu, B. Cordell, Positive and negative regulation of APP amyloidogenesis by sumoylation, Proc. Natl. Acad. Sci. USA 100 (2003) 259–264, https://doi.org/10.1073/pnas.0235361100.

[32] L. Fioriti, N. Wijesekara, E.K. Argyrousi, S. Matsuzaki, H. Takamura, K. Satoh, K. Han, H. Yamauchi, A. Staniszewski, E. Acquarone, F. Orsini, A. Martucci, T. Katayama, O. Arancio, P.E. Fraser, Genetic and pharmacologic enhancement of SUMO2 conjugation prevents and reverses cognitive impairment and synaptotoxicity in a preclinical model of Alzheimer's disease, Alzheimers Dement. 21 (2025) e70030, https://doi.org/10.1002/alz.70030.

[33] Y. Perez-Riverol, C. Bandla, D.J. Kundu, S. Kamatchinathan, J. Bai, S. Hewapathirana, N.S. John, A. Prakash, M. Walzer, S. Wang, J.A. Vizcaíno, The PRIDE database at 20 years: 2025 update, Nucleic Acids Res. 53 (D1) (2025) D543–D553, https://doi.org/10.1093/nar/gkae1011.

[34] M.J.E. Fischer, Amine coupling through EDC/NHS: a practical approach, in: N. J. Mol, M.J.E. Fischer (Eds.), Surface Plasmon Resonance: Methods and Protocols, Humana Press, Totowa, NJ, 2010, pp. 55–73, https://doi.org/10.1007/978-1-60761-670-2_3.

[35] J.G. Quinn, Modeling taylor dispersion injections: determination of kinetic/affinity interaction constants and diffusion coefficients in label-free biosensing, Anal. Biochem. 421 (2012) 391–400, https://doi.org/10.1016/j.ab.2011.11.024.

[36] S. Zimbone, M.L. Giuffrida, M.F.M. Sciacca, R. Carrotta, F. Librizzi, D. Milardi, G. Grasso, A VEGF fragment encompassing residues 10–30 inhibits Aβ1–42 amyloid aggregation and exhibits neuroprotective properties matching the full-length protein, ACS Chem. Neurosci. 15 (2024) 4580–4590, https://doi.org/10.1021/acschemneuro.4c00669.

[37] F. Fiumara, L. Fioriti, E.R. Kandel, W.A. Hendrickson, Essential role of coiled coils for aggregation and activity of Q/N-rich prions and polyQ proteins, Cell 143 (2010) 1121–1135, https://doi.org/10.1016/j.cell.2010.11.042.

[38] M. Békés, J. Prudden, T. Srikumar, B. Raught, M.N. Boddy, G.S. Salvesen, The dynamics and mechanism of SUMO chain deconjugation by SUMO-specific proteases, J. Biol. Chem. 286 (2011) 10238–10247, https://doi.org/10.1074/jbc.M110.205153.

[39] F. Bellia, V. Lanza, S. García-Viñuales, I.M.M. Ahmed, A. Pietropaolo, C. Iacobucci, G. Malgieri, G. D'Abrosca, R. Fattorusso, V.G. Nicoletti, D. Sbardella, G.R. Tundo, M. Coletta, L. Pirone, E. Pedone, D. Calcagno, G. Grasso, D. Milardi, Ubiquitin binds the amyloid β peptide and interferes with its clearance pathways, Chem. Sci. 10 (2019) 2732–2742, https://doi.org/10.1039/c8sc03394c.

[40] E.S. Soares, A.C.G. de Souza, C.A. Zanella, R.E. Carmichael, J.M. Henley, K. A. Wilkinson, H.I. Cimarosti, Effects of amyloid-β on protein SUMOylation and levels of mitochondrial proteins in primary cortical neurons, IBRO Neurosci. Rep. 12 (2022) 142–148, https://doi.org/10.1016/j.ibneur.2022.01.003.

[41] M.S. Rodriguez, C. Dargemont, R.T. Hay, SUMO-1 conjugation *in vivo* requires both a consensus modification motif and nuclear targeting, J. Biol. Chem. 276 (2001) 12654–12659.

[42] I. Matic, J. Schimmel, I.A. Hendriks, M.A. van Santen, F. van de Rijke, H. van Dam, F. Gnad, M. Mann, A.C. Vertegaal, Site-specific identification of SUMO-2 targets in cells reveals an inverted SUMOylation motif and a hydrophobic cluster SUMOylation motif, Mol. Cell 39 (2010) 641–652.

[43] I.A. Hendriks, D. Lyon, C. Young, L.J. Jensen, A.C.O. Vertegaal, M.L. Nielsen, Site-specific mapping of the human SUMO proteome reveals co-modification with phosphorylation, Nat. Struct. Mol. Biol. 24 (2017) 325–336, https://doi.org/10.1038/nsmb.3366.

[44] M.H. Tatham, E. Jaffray, O.A. Vaughan, J.M.P. Desterro, C.H. Botting, J. H. Naismith, R.T. Hay, Polymeric chains of SUMO-2 and SUMO-3 are conjugated to protein substrates by SAE1/SAE2 and Ubc9, J. Biol. Chem. 276 (2001) 35368–35374, https://doi.org/10.1074/jbc.M104214200.

[45] K. Wagner, K. Kunz, T. Piller, G. Tascher, S. Hölper, P. Stehmeier, J. Keiten-Schmitz, M. Schick, U. Keller, S. Müller, The SUMO isopeptidase SENP6 functions as a rheostat of chromatin residency in genome maintenance and chromosome dynamics, Cell Rep. 29 (2019) 480–494.

[46] K. Sokratous, L.V. Roach, D. Channing, J. Strachan, J. Long, M.S. Searle, R. Layfield, N.J. Oldham, Probing affinity and ubiquitin linkage selectivity of ubiquitin-binding domains using mass spectrometry, J. Am. Chem. Soc. 134 (2012) 6416–6424, https://doi.org/10.1021/ja300749d.

[47] N. Nagaraj, J.R. Wisniewski, T. Geiger, J. Cox, M. Kircher, J. Kelso, S. Pääbo, M. Mann, Deep proteome and transcriptome mapping of a human cancer cell line, Mol. Syst. Biol. 7 (2011) 548, https://doi.org/10.1038/msb.2011.81.

[48] A. Vertegaal, S. Ogg, E. Jaffray, M.S. Rodríguez, R. Hay, J. Andersen, M. Mann, A. Lamond, A proteomic study of SUMO-2 target proteins, J. Biol. Chem. 279 (2004) 33791–33798, https://doi.org/10.1074/JBC.M404201200.

[49] Linda Lee, Mikako Sakurai, Shinsuke Matsuzaki, Ottavio Arancio, Paul Fraser, SUMO and Alzheimer's disease, Neuromolecular Med. 15 (4) (2013 Dec), https://doi.org/10.1007/s12017-013-8257-7, 720-36. Epub 2013 Aug 25.